Acoustical properties of $(TMTSF)_2PF_6$ in the spin-density-wave ground state

S. Zherlitsyn
Physikalisches Institut, Universität Frankfurt, D-60054 Frankfurt, Germany
and Institute for Low Temperature Physics & Engineering, 310164 Kharkov, Ukraine

G. Bruls
Physikalisches Institut, Universität Frankfurt, D-60054 Frankfurt, Germany

A. Goltsev
Ioffe Physical-Technical Institute, 194021 St. Petersburg, Russia

B. Alavi
Department of Physics, University of California, Los Angeles, California 90095-1547

M. Dressel
I. Physikalisches Institut, Universität Stuttgart, D-70550 Stuttgart, Germany
(Received 4 June 1998; revised manuscript received 23 November 1998)

We have carried out ultrasonic investigations of $(TMTSF)_2PF_6$ in the spin-density-wave (SDW) ground state. Some features for the elastic behavior of the SDW state are found. One of the acoustic modes shows a jump in the sound velocity at the critical temperature of the SDW transition ($T_{SDW}\approx 12$ K) and a relaxation peak in the attenuation of sound just below T_{SDW}. From this peak we have estimated the characteristic relaxation time of the spin fluctuations along the b axis to be $t_0=2\times10^{-11}$ s. The sound velocity of another acoustic mode changes with temperature as the square of the order parameter. Besides a maximum just below T_{SDW} the attenuation of this mode has an exponential behavior at low temperatures and yields an energy gap value equal to $2\Delta(0)\approx 96$ K, which is much larger than the BCS value $2\Delta(0)\approx 43$ K. In addition there is an acoustic mode which displays a slow decrease of the sound velocity in the SDW state. We have also studied the influence of a magnetic field applied along the c^* axis on the acoustic properties of $(TMTSF)_2PF_6$: T_{SDW} increases in the magnetic field. We discuss our experimental results in the frame of theoretical considerations which are based on the assumption that phonons influence the exchange interaction between the spins of the conducting electrons and thus couple to the SDW (magnetoelastic coupling). In our model, the temperature behavior of the sound velocity and the attenuation of sound is related to the real and imaginary parts of the dynamical spin susceptibility. This model allows us to classify the temperature behavior of different acoustic modes and to explain the observed anomalies in the sound velocity and the attenuation of sound in the SDW ground state. [S0163-1829(99)06821-6]

I. INTRODUCTION

One-dimensional electron systems are of great theoretical importance[1,2] because the reduced dimensionality leads to a number of interesting ground states like charge density waves (CDW), spin density waves (SDW), or spin Peierls (SP). Since their discovery twenty years ago, the Bechgaard salts $(TMTSF)_2X$, where TMTSF is tetramethyl-tetraselenafulvalene and X stands for a monovalent anion like AsF_6, PF_6, or ClO_4 and their sulfur analogs $(TMTTF)_2X$ became the prime examples of quasi-one-dimensional materials and an enormous amount of experimental data has been accumulated over the years; for reviews see Refs. 3 and 4.

$(TMTSF)_2PF_6$ has a triclinic crystal structure with a $P\bar{1}$ symmetry ($a=7.297$ Å, $b=7.711$ Å, $c=13.522$ Å, $\alpha=83.39°$, $\beta=86.27°$, $\gamma=71.01°$). The organic cathions TMTSF are stacked along the a direction, b' is perpendicular to a, and c^* is normal to the ab' plane. At room temperature $(TMTSF)_2PF_6$ is highly conducting along the chain direction with an anisotropy of several orders of magnitude. Cooling down at ambient pressure it undergoes a metal-to-insulator transition at $T_{SDW}\approx 12$ K to a SDW ground state, i.e., it becomes an itinerant antiferromagnet. Due to the instability of the low-dimensional electron gas a gap opens at the Fermi surface. In contrast to a CDW transition, no structural changes are observed.[3] For the thermal expansion $\Delta a/a$ of $(TMTSF)_2PF_6$ within a few parts in 10^{-8} no change was found at T_{SDW},[5] indicating that the spin-lattice coupling in the SDW state is very weak. However, this does not mean the coupling is negligible. For instance, the missing spectral weight of the collective phason excitation observed in the SDW state[6] may be explained by the electron-phonon coupling leading to an enhanced mass of the condensate. In order to address the coupling issue we have performed ultrasonic measurements on $(TMTSF)_2PF_6$ in the temperature range around the SDW transition.

We present results of high frequency ultrasonic investigations of single crystal $(TMTSF)_2PF_6$ in the temperature range $2\text{ K}<T<40$ K. Due to the small size of the crystals, acoustical studies of the organic compound $(TMTSF)_2X$ have

been limited in number. To our knowledge only low-frequency vibrating-reed technique measurements have been performed[7–11] where an anomalous behavior of sound velocity and internal friction was observed below the critical temperature ($T_{SDW} \sim 12$ K) of the SDW phase transition. The temperature dependencies of these characteristics were theoretically discussed in a number of papers.[12–14] Specifically the hardening of the elastic constants below T_{SDW} was ascribed to the reduction in the quasiparticle screening of the ion potential due to the formation of the SDW state. Another possible mechanism is a finite magnon-phonon coupling. One important point in these considerations is whether the SDW is pinned (without depinning electrical field, it is). Measurements of the Youngs' modulus under external bias were performed to explore these phenomena.[8,11] Virosztek and Maki[14] predict a coupling of only the transverse sound wave with displacement vector parallel to the chain direction to the phason of the spin density wave. Due to this fact the relative change of the longitudinal sound velocity below T_{SDW} should be a factor 10^2 smaller than for the velocity of the transverse sound wave.

In addition to the small size of the sample, performing and analyzing the experiments is complicated by the fact that $(TMTSF)_2PF_6$ has a triclinic crystal symmetry with nonorthogonal crystal axes. Only the long axis of the sample coincides with the real crystallographic *a* axis (the direction along the spin chains). The *b* and *c* axes have some nonzero angle (see above) with the normal directions of the as-grown crystal surfaces. Under these circumstances the experimentally excitable sound waves are mainly in combinations not even representing pure (longitudinal or transverse) modes. In practice, it means that our transverse (shear) transducers will excite also (quasi)longitudinal sound modes and vice versa.

II. EXPERIMENTAL TECHNIQUE AND RESULTS

The crystal used in our study had a size of $2 \times 0.7 \times 0.3\,\text{mm}^3$ with the crystallographic *a* axis directed along the largest dimension. We utilized resonant $LiNbO_3$ ultrasound transducers with a fundamental frequency of 70 MHz. In order to reduce the possibility of a bond break we used a thin mylar film (thickness 10 μm) as a buffer between the sample and the transducers. Sputtered aluminum film on the mylar served as the electrical ground contact for the transducers. The transducers and the mylar film were glued to the as-grown planes normal to c^* with a liquid polymer (Thiokol LP-32). The geometry of the sound excitation is shown in Fig. 1. In case of the transverse transducers the polarization **e** was along the *a* axis. We performed measurements of the sound velocity and the attenuation of ultrasound both at the fundamental frequency of the transducers and at the third harmonic. The ultrasonic pulse technique used is described elsewhere.[15]

In case of triclinic symmetry there are 21 independent elastic moduli and in general the modes propagating along the crystal axes are neither purely longitudinal nor purely transverse. However, it is well known that there are three independent acoustic waves with different velocity for any crystallographic direction in a crystal, and the particle displacements for these modes are perpendicular to each other.[16] In the case of triclinic symmetry there is a nonzero,

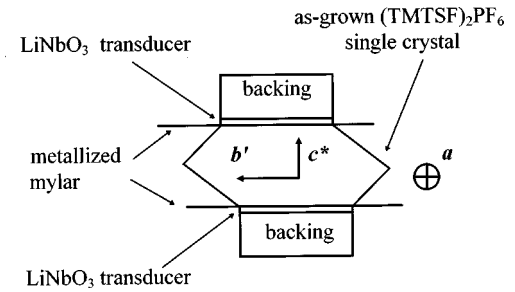

FIG. 1. Sketch of the geometry used to explain the excitation of the ultrasound waves in $(TMTSF)_2PF_6$. Metallized mylar was used as a buffer. Two resonance $LiNbO_3$ transducers and a mylar film were glued to the as-grown surfaces normal to the c^* axis. In case of the transverse transducers the polarization vector was directed along the *a* axis. The *a* axis is perpendicular to the b'-c^* plane.

respectively non-90°, angle between the wave vector **q** and the polarization vector **e** for each mode taken separately. Here, we do not consider the exceptional occurrence of pure modes due to special relations between the elastic constants.[17] Thus we assume that one quasi-longitudinal and two quasi-transverse modes exist for each direction in a triclinic system. The receiving ultrasonic transducer picks up signals from all these modes. The situation becomes more complicated because of the small size of the sample (along the selected c^* crystallographic direction) and a possibility of interference between the acoustic waves reflected from the sample surfaces. For our investigation we used short (<100 ns) ultrasonic pulses. That allows us to separate temporally the different signals in the receiving part of the setup. These signals are associated with different acoustic modes in the crystal. They were stable below 50 K and we could observe different types of temperature behavior for the sound velocity and the attenuation of sound for them.

Using longitudinal transducers glued on as-grown crystal surfaces normal to c^* (see Fig. 1), we observed a few signals separated in time, which are related to different acoustic modes of the triclinic crystal. The modes demonstrate different temperature dependencies of the velocity and the attenuation below T_{SDW}. In Fig. 2 we present the behavior of one of these modes (called mode I) that is similar to the results observed by using vibrating-reed technique.[7–9] Apart from this type of temperature behavior, we discovered completely different temperature dependencies of the ultrasonic velocity and attenuation for other modes. They are shown in Figs. 3 and 4 and called mode II and mode III, respectively. Using transverse transducers with the polarization vector along the *a* axis gives one more type of temperature behavior (probably a mixed mode, see Fig. 5) for the velocity of sound and the attenuation. Such kind of behavior represented in Figs. 3–5 has never been theoretically discussed for SDW phase transition in quasi-one-dimensional conductors like $(TMTSF)_2PF_6$. However, the steplike behavior is very common for a second order phase transition which exhibits a linear coupling of the strain to the square of the order parameter.[18] It is also observed for a CDW transition, for instance in the quasi-one-dimensional metal blue bronze.[19] One can note that while it is well known that a CDW is associated with a lattice distortion, this is not so obvious in the case of a SDW in itinerant electron systems. Within our

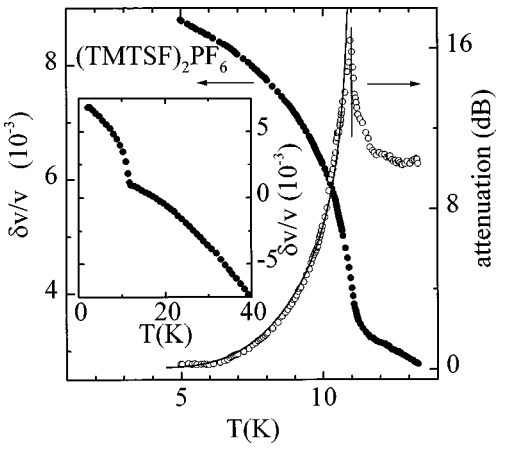

FIG. 2. Temperature behavior of the sound velocity (filled circles) and the attenuation (open circles) of sound for the quasi-transverse acoustic mode (mode I) in $(TMTSF)_2PF_6$. Longitudinal ultrasonic transducers ($\mathbf{q}\|\mathbf{e}\|c^*$) were used at a frequency $f = 199$ MHz. The solid lines represent the BCS-like behavior of the attenuation according to Eq. (33). The best fit gives a value of 96 K for the single particle gap $2\Delta(0)$. The inset shows the temperature dependence of the sound velocity up to 40 K.

experimental accuracy, we did not detect any hysteresis at the SDW phase transition and hence no indication for a possible first-order character of the transition.

Owing to the low triclinic symmetry of $(TMTSF)_2PF_6$ there is an angle between phase and group velocity of the sound waves which traverse the crystal. Since the elastic constants change at the phase transition, the angle may also change. In principle, this effect must be taken into account when analyzing the data on the sound attenuation. However, this effect is sufficiently small, because the relative change of the angle is proportional to a relative change of the sound velocity. In our case the latter has a value of about 10^{-3}. Hence, the relative change of the angle is also of the order of 10^{-3} and can explain only about 1% of the observed change in the sound attenuation. Therefore we can neglect this effect.

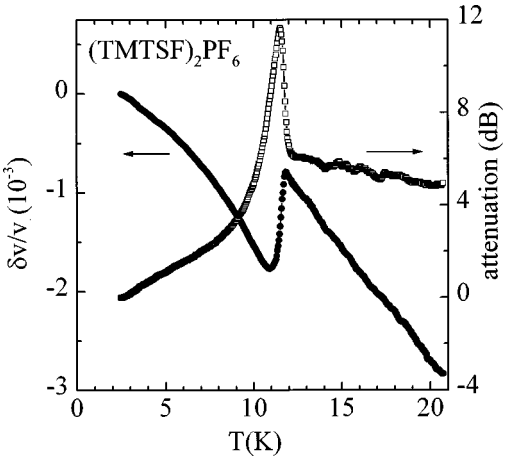

FIG. 3. Sound velocity (filled circles) and the sound attenuation (open squares) versus temperature for the quasilongitudinal acoustic mode (mode II) in $(TMTSF)_2PF_6$. Longitudinal transducers ($\mathbf{q}\|\mathbf{e}\|c^*$) were used at a frequency of 204 MHz. The lines connect the experimental points.

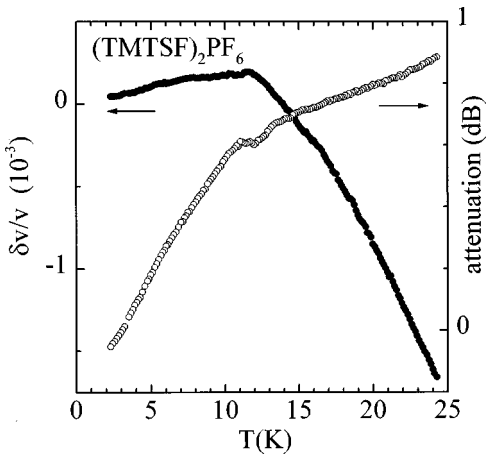

FIG. 4. Temperature behavior of the sound velocity (filled circles) and the attenuation (open circles) of sound for the quasi-transverse acoustic mode (mode III) in $(TMTSF)_2PF_6$. Longitudinal ultrasonic transducers ($\mathbf{q}\|\mathbf{e}\|c^*$) were used at a frequency of 66 MHz.

It is known from the different experiments (Refs. 20 and 21 and references therein) that there is an additional transition in $(TMTSF)_2PF_6$ at approximately 3.5 K. As it was suggested, the energy gap does not open completely at T_{SDW} and below this temperature both the normal charge carriers and the SDW coexist,[20,21] the complete opening of the gap over the Fermi surface occurs in $(TMTSF)_2PF_6$ at 3.5 K. The suggestion that at the SDW transition the energy gap at the Fermi level opens only partially stands in contrast to the strong increase of the resistivity at T_{SDW},[4] and the rapid vanishing of the EPR signal related to the conduction electrons.[22,23] The negligible change of the optical properties at the SDW transition along the chains, however, may indicate that a part of the normal electrons remains below T_{SDW} (Ref. 6) (to our knowledge, no optical measurements have been performed below 4 K). In particular magnetotransport and Hall-effect measurements indicate a strong coupling of

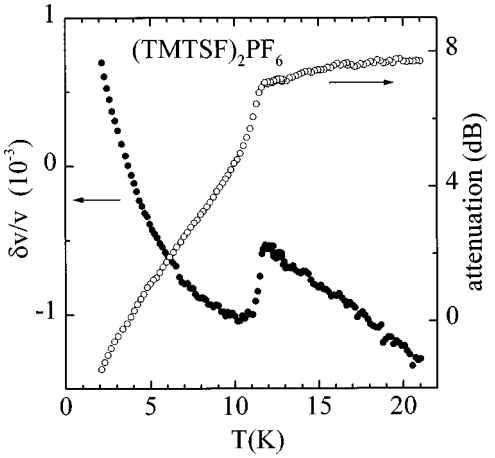

FIG. 5. Temperature behavior of the sound velocity (filled circles) and the attenuation (open circles) of sound for the mode that shows a behavior which is a mixture of mode I, mode II, and mode III, with a sign reversal of the mode I and mode III coefficients (see text). Transverse ultrasonic transducers ($\mathbf{q}\|c^*, \mathbf{e}\|a$) were used at a frequency of 71 MHz.

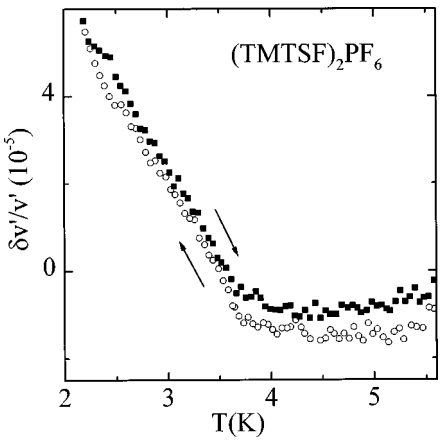

FIG. 6. Temperature dependence of the sound velocity of the acoustic mode II (see Fig. 3) in the vicinity of the low temperature transition between different SDW phases in $(TMTSF)_2PF_6$. A parabolic background was subtracted (see text). Temperature sweep up (filled squares) and sweep down (open circles) are shown.

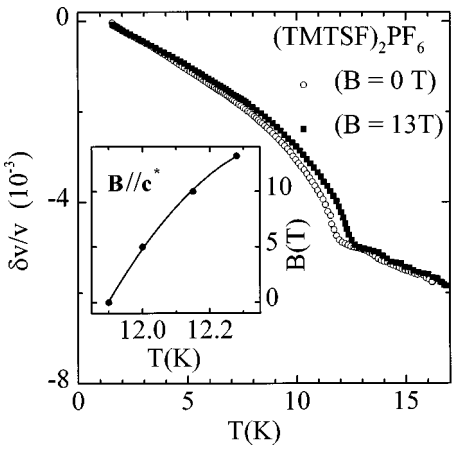

FIG. 7. Temperature behavior of the sound velocity for mode I (see Fig. 2) measured with and without magnetic field applied along the c^* direction. The open circles correspond to $B=0$ T and the filled squares correspond to $B=13.2$ T. The inset shows a part of the B-T phase diagram. The points were extracted from the ultrasonic data. The line was drawn to guide the eye.

the SDW and the normal electrons.[24,25] As discussed for instance in Ref. 21, the partial opening of the gap could be related to an incommensurate nesting vector. A completely alternative picture with respect to the 3.5 K anomalies, emerging from dielectric constant and heat capacity measurements,[26–28] is a glass transition. In our ultrasound experiments we observe a slight anomaly in the sound velocity of the acoustic mode II shown in Fig. 3. In order to extract this anomaly we made a second order polynomial fit of the temperature dependence of the sound velocity at the temperature range between 5 and 9 K. Then we subtracted a low temperature extrapolation of this polynomial fit from the data. The result is shown in Fig. 6. This additional term of the sound velocity exhibits a clear kink at a temperature of about 3.5 K. The nonexponential temperature behavior of the attenuation of sound observed for some of the acoustic modes below T_{SDW} is typical for a gap-anisotropic system with nodes. Therefore the kink could be an indication of a phase transition between incommensurate and commensurate SDW phases below which the gap opens over the complete Fermi surface.

We investigated the influence of an external magnetic field up to 13 T, applied along the magnetically hard c^* axis, on the acoustic properties of $(TMTSF)_2PF_6$. We did not notice any significant anomalies in the field dependencies of the sound velocity and the attenuation of sound in the temperature range $2\ \mathrm{K}<T<14\ \mathrm{K}$. However the temperature dependencies measured at different applied magnetic fields display a shift of T_{SDW} as a function of magnetic field. Figure 7 shows the temperature dependence of mode I in Fig. 2 measured for $B=0$ T and $B=13.2$ T. The inset of Fig. 7 exhibits a part of the B-T phase diagram obtained from our ultrasonic data. This phase diagram is consistent with the one proposed by other groups[21,29–31] who observed and explained a quadratic field dependence of the T_{SDW}.

III. THEORY

In order to explain the origin of the different temperature dependencies of the acoustic modes observed at $T<T_{\mathrm{SDW}}$ it is necessary to have a model of the electron-phonon coupling in $(TMTSF)_2PF_6$. The model of the electron-phonon coupling proposed in a number of works[12–14] does not allow to describe all observed anomalies. The temperature behavior of the sound velocity displayed in Fig. 2 is in qualitative agreement with this model. However, the jump in the sound velocity and the sharp peak in the attenuation presented in Fig. 3, as well as the temperature behavior of the velocity and the attenuation of the acoustic mode in Fig. 4 are not explained. In order to account for our data, we have to assume that there is an additional mechanism of electron-phonon coupling active in $(TMTSF)_2PF_6$. In the present section we consider a microscopic model of magnetoelastic coupling that allows us to explain the observed peculiarities of the acoustic modes.

In quasi-one-dimensional conductors both intrachain and interchain exchange interactions between conduction electrons play an important role in the formation of the different ground states (see, for example, Refs. 4, 1, and 32). One can write the exchange interactions in the general form:

$$H_{\mathrm{exc}}=\sum_{\mathbf{p},\mathbf{p}',\mathbf{k}}\sum_{\alpha\beta\gamma\delta} G(\mathbf{p}-\mathbf{k},\alpha;\mathbf{p}'+\mathbf{k},\gamma;\mathbf{p}',\delta;\mathbf{p},\beta)\,a^{+}_{\mathbf{p}-\mathbf{k},\alpha}a^{+}_{\mathbf{p}'+\mathbf{k},\gamma}a_{\mathbf{p}',\delta}a_{\mathbf{p},\beta}, \quad (1)$$

where, for instance, $a^{+}_{\mathbf{p}-\mathbf{k},\alpha}$ and $a_{\mathbf{p}',\delta}$ are the operators of creation and annihilation of the conduction electrons in a state with momentum $\mathbf{p}-\mathbf{k}$ and spin α and a state with momentum $\mathbf{p}'$ and spin δ, respectively. The dependence of the exchange constant G on momenta and spin indices is determined by both the lattice anisotropy and the magnetic anisotropy. The latter, for example, is related to the spin-orbital interaction. It is known that $(TMTSF)_2PF_6$ has anisotropic magnetic properties[4,33] with similarities to an ordinary antiferromagnet below T_{SDW}. The easy, intermediate, and hard axes are located approximately along the b, a, and c axes, respectively. One can suppose that phonons having wave

vector $\mathbf{q}$ and producing the strain ε_{ij}, $i,j=x,y$ or z, influence the exchange interactions:

$$\delta H_{\rm exc}=\sum_{\mathbf{p},\mathbf{p}',\mathbf{k},\mathbf{q}}\sum_{\alpha\beta\gamma\delta} G_{ij}(\mathbf{p}-\mathbf{k}+\mathbf{q},\alpha;\mathbf{p}' +\mathbf{k},\gamma;\mathbf{p}',\delta;\mathbf{p},\beta)\varepsilon_{ij}(\mathbf{q})a^{+}_{\mathbf{p}-\mathbf{k}+\mathbf{q},\alpha}a^{+}_{\mathbf{p}'+\mathbf{k},\gamma}a_{\mathbf{p}',\delta}a_{\mathbf{p},\beta}, \tag{2}$$

where $\varepsilon_{ij}(\mathbf{q})$ is the Fourier transform of the strain and is related to the phonon creation and annihilation operators $b^{+}_{\mathbf{q}}$ and $b_{\mathbf{q}}$, respectively, in the conventional way:

$$\varepsilon_{ij}(\mathbf{q})=\frac{i}{2}\left(\frac{\hbar}{2M\omega_q}\right)^{1/2}(q_ie_j+q_je_i)(b_{\mathbf{q}}+b^{+}_{-\mathbf{q}}),$$

where $\mathbf{e}$ is the polarization vector, ω_q is the frequency of the acoustic wave, and M is the ion mass. Unfortunately, the Hamiltonian (2) is too complicated to be used for our specific aims. It is very difficult to perform a complete analysis of the influence of the electron-phonon coupling (3) on the acoustic modes due to the low triclinic symmetry of $(TMTSF)_2PF_6$. Most of the dominant physical features of acoustic measurements may be explained by assuming an orthorhombic system; thus for the further discussion $b'=b$ and $c^*=c$.

Based on symmetry considerations and neglecting the dependence of G on momenta we represent the Hamiltonian (2) in the form of a magneto-elastic spin Hamiltonian:

$$H'_{\rm exc}=\sum_{\mathbf{k},\mathbf{q}}\left\{\sum_{ij} G^i_j\varepsilon_{jj}(\mathbf{q})S_i(\mathbf{k}-\mathbf{q})S_i(-\mathbf{k}) +\frac{1}{2}\sum_{i\neq j} G_{ij}\varepsilon_{ij}(\mathbf{q})S_i(\mathbf{k}-\mathbf{q})S_j(-\mathbf{k})\right\}, \tag{3}$$

where

$$S_i(\mathbf{k})=\frac{1}{2}\sum_{\mathbf{p}\alpha\beta} a^{+}_{\mathbf{p}-\mathbf{k},\alpha}\sigma^i_{\alpha\beta}a_{\mathbf{p},\beta} \tag{4}$$

is the Fourier transform of the spin density operator $S_i(\mathbf{r})=\frac{1}{2}\Sigma_{\alpha\beta}a^{+}_{\alpha}(\mathbf{r})\sigma^i_{\alpha\beta}a_{\beta}(\mathbf{r})$ of the conduction electrons, and $\sigma^i_{\alpha\beta}$ are the Pauli matrices, with $i=x,y,z$. The Hamiltonian $H'_{\rm exc}$ is an approximate representation of $H_{\rm exc}$, because there are some terms omitted (the problems with transforming an exchange Hamiltonian into a spin Hamiltonian have been discussed by Herring[34]). The magnetic properties of $(TMTSF)_2PF_6$ have been sussesfully described using an effective Heisenberg Hamiltonian.[32] Therefore we expect the magnetoelastic spin Hamiltonian of Eq. (3) to be appropriate also. In the Hamiltonian (3) one can group the components of strains ε_{ij} to form irreducible representations of the orthorhombic group. Then the Hamiltonian (3) can be represented as a sum over the representations (see, for example, review[35]). However, it makes $H'_{\rm exc}$ to be complicated and inconvenient for the purpose of the paper. Equation (3) describes a magnetoelastic coupling between electron spins and strains like it has been discussed for ferromagnetic and antiferromagnetic crystals.[36]

We begin with a longitudinal acoustic mode propagating along the i axis, $i=a$, b or c. The theoretical result for this mode will turn out to fit the steplike behavior of Fig. 3 (i.e., mode II) quite well. The coupling of the mode to the spin density of conduction electrons contains the following terms:

$$E_l(\varepsilon_{ij})=\varepsilon_{ii}(\mathbf{q})\sum_{\mathbf{k},\mathbf{q}}\sum_j G^i_jS_j(\mathbf{k}-\mathbf{q})S_j(-\mathbf{k}). \tag{5}$$

Apart from the electron-phonon coupling the behavior of the electron subsystem is governed by the conventional Hamiltonian H_0.[1] We will suppose that below the critical temperature $T_{\rm SDW}$ a SDW state with a nesting vector $\mathbf{Q}$ is formed,[37] with the spins of the conduction electrons directed along the b axis:

$$\langle S_b(\mathbf{r})\rangle=\langle S_b(\mathbf{Q})\rangle\exp(i\mathbf{Q}\cdot\mathbf{r})+\langle S(-\mathbf{Q})\rangle\exp(-i\mathbf{Q}\cdot\mathbf{r}) =S_b(T)\cos(\mathbf{Q}\cdot\mathbf{r}+\varphi), \tag{6}$$

where $S_b(T)$ is the temperature dependent amplitude of the spin-density wave. It is well known that $S_b(T)$ is proportional to the energy gap which opens at the Fermi surface and thus to the order parameter. Using the Matsubara method in the second order of the coupling constants G^j_i, we find that at $T<T_{\rm SDW}$ the coupling (5) gives two contributions to the elastic constant c_{ii}:

$$\Delta c_{ii}=\Delta c^{(1)}_{ii}+\Delta c^{(2)}_{ii},$$

$$\Delta c^{(1)}_{ii}=-4(G^i_b)^2S^2_b(T)\chi'_{bb}(\mathbf{Q}+\mathbf{q},\omega_q), \tag{7}$$

$$\Delta c^{(2)}_{ii}=-4\sum_j (G^i_j)^2Y'_{jj}(q,\omega_q), \tag{8}$$

where $\chi'_{bb}(\mathbf{Q}+\mathbf{q},\omega_q)$ is the real part of the longitudinal susceptibility $\chi_{bb}(\mathbf{p},\omega)=\beta\langle S_b(\mathbf{p},\omega)S_b(-\mathbf{p},-\omega)\rangle$ at $\mathbf{p}=\mathbf{Q}+\mathbf{q}$ and $\omega=\omega_{\mathbf{q}}$. The function $Y_{ij}(q,\omega_q)$ is a four-spin correlation function, $Y'_{jj}(q,\omega_q)=\mathrm{Re}\,Y_{jj}(q,\omega_q)$. We approximate the four-spin correlation function by a product of two-spin correlation functions. As a result we obtain

$$Y_{ij}(q,\omega_q)\equiv\lim_{i\omega_n\to\omega_q+i\varepsilon} T\sum_{\mathbf{k}}\sum_{i\omega}\chi_{ii}(\mathbf{k}-\mathbf{q},i\omega-i\omega_n)\times\chi_{jj}(\mathbf{k},i\omega),$$

$$\mathrm{Re}\,Y_{ij}(q,\omega)=\frac{1}{2\pi}\sum_{\mathbf{k}}\int_{-\infty}^{\infty}d\varepsilon\coth\left(\frac{\varepsilon}{2T}\right) \times\{\chi''_{ii}(\mathbf{k}-\mathbf{q},\varepsilon)\chi'_{jj}(\mathbf{k},\varepsilon+\omega_q) +\chi'_{ii}(\mathbf{k}-\mathbf{q},\varepsilon-\omega_q)\chi''_{jj}(\mathbf{k},\varepsilon)\},$$

$$\mathrm{Im}\,Y_{ij}(q,\omega)=\frac{1}{2\pi}\sum_{\mathbf{k}}\int_{-\infty}^{\infty}d\varepsilon\coth\left(\frac{\varepsilon}{2T}\right) \times\{\chi''_{ii}(\mathbf{k}-\mathbf{q},\varepsilon)\chi''_{jj}(\mathbf{k},\varepsilon+\omega_q) -\chi''_{ii}(\mathbf{k}-\mathbf{q},\varepsilon-\omega_q)\chi''_{jj}(\mathbf{k},\varepsilon)\}. \tag{9}$$

The electron-phonon coupling (3) gives an additional contribution to the attenuation of the longitudinal acoustic waves:

$$\alpha_{ii}=\alpha^{(1)}_{ii}+\alpha^{(2)}_{ii},$$

$$\alpha_{ii}^{(1)}=\frac{4\omega_q}{Mv_l^3}(G_b^i)^2S_b^2(T)\chi''_{bb}(\mathbf{Q}+\mathbf{q},\omega_q), \tag{10}$$

$$\alpha_{ii}^{(2)}=\frac{4\omega_q}{Mv_l^3}\sum_j (G_b^i)^2Y''_{jj}(q,\omega_q), \tag{11}$$

where v_l is the velocity of the longitudinal acoustic wave, $\chi''_{bb}(\mathbf{Q}+\mathbf{q},\omega_q)=\mathrm{Im}\,\chi_{bb}(\mathbf{Q}+\mathbf{q},\omega_q)$ and $Y''_{jj}(q,\omega_q)=\mathrm{Im}\,Y_{jj}(q,\omega_q)$. In the paramagnetic phase, i.e., at $T>T_{\mathrm{SDW}}$, the $\alpha_{ii}^{(1)}$ and $\Delta c_{ii}^{(1)}$ are equal to zero since $S_b(T)=0$. Therefore, only $\Delta c_{ii}^{(2)}$ and $\alpha_{ii}^{(2)}$ contribute to the elastic constants and the attenuation, respectively. At $T<T_{\mathrm{SDW}}$ both contributions must be taken into account.

For understanding the results represented by Eqs. (7) and (8) it is necessary to note that in accordance with Eq. (5) the strain ε_{ii} is coupled linearly to the square of the order parameter S_b^2. Equations (7) and (8) are the conventional equations for this kind of coupling.[18] The contributions $\Delta c_{ii}^{(2)}$ and $\alpha_{ii}^{(2)}$ are due to spin fluctuations.

From Eqs. (7)–(11) it follows that the temperature behavior of the elastic constants and the attenuation are determined by the temperature dependence of the dynamical susceptibility $\chi_{ii}(\mathbf{k},\omega)$. However, unlike $\alpha_{ii}^{(1)}$ and $\Delta c_{ii}^{(1)}$, which are determined by the staggered susceptibility at $\mathbf{k}\approx\mathbf{Q}$ and $\omega=\omega_q$, the terms $\Delta c_{ii}^{(2)}$ and $\alpha_{ii}^{(2)}$ are determined by a complete dependence of $\chi_{jj}(\mathbf{k},\omega)$ on $\mathbf{k}$ and ω in the whole $\mathbf{k}-\omega$ space.

Now we will study the temperature behavior of $\alpha_{ii}^{(1)}$ and $\Delta c_{ii}^{(1)}$. In case of the itinerant antiferromagnet $(\mathrm{TMTSF})_2\mathrm{PF}_6$, below T_{SDW}, the imaginary and the real parts of the longitudinal susceptibility at small frequencies ω and wave vectors $\mathbf{k}$ near $\pm\mathbf{Q}$, i.e., $\mathbf{k}=\pm\mathbf{Q}-\mathbf{q}$, have the form[38,39]

$$\chi''_{bb}(\mathbf{Q}+\mathbf{q},\omega)=\frac{A\omega t}{\tau[(1+\xi_i^2q_i^2)^2+t^2\omega^2]}, \tag{12}$$

$$\chi'_{bb}(\mathbf{Q}+\mathbf{q},\omega)=\frac{B(1+\xi_i^2q_i^2)}{\tau[(1+\xi_i^2q_i^2)^2+t^2\omega^2]}, \tag{13}$$

where $\tau=1-T/T_{\mathrm{SDW}}$ is the reduced temperature, $\xi_i=\xi_{0,i}\tau^{-1/2}$ is the correlation length in the i direction ($i=a$, b and c), $t=t_0\tau^{-1}$ is a characteristic time, and A and B are smooth functions of temperature. The expression (12) was used successfully[38] for explaining the singular profile of the nuclear relaxation rate T_1^{-1} in $(\mathrm{TMTSF})_2\mathrm{PF}_6$. For a sufficiently broad temperature region near T_{SDW} but not too close to T_{SDW} we have $\xi_q\ll 1$, i.e., the acoustic wave length is much larger than the correlation length while $t\omega_q$ may be arbitrary. Then Eqs. (7) and (13) give

$$\Delta c_{ii}^{(1)}=-[4(G_b^i)^2S_b^2(T)\tau^{-1}B]\frac{1}{1+t^2\omega_q^2}. \tag{14a}$$

Close to T_{SDW} the characteristic time $t=t_0\tau^{-1}$ is large and $t\omega_q\gg 1$, therefore, at $T=T_{\mathrm{SDW}}$ we have $\Delta c_{ii}^{(1)}=0$. With decreasing temperature the characteristic time t decreases very quickly and $t\omega_q$ becomes small. In the temperature region where $t\omega_q\ll 1$, the terms $\Delta c_{ii}^{(1)}$ have the following temperature behavior:

$$\Delta c_{ii}^{(1)}(T)=-4(G_b^i)^2S_b^2(T)\tau^{-1}B. \tag{14b}$$

From the experimental data[40,41] one can see that at T close to T_{SDW} the square of the order parameter has a linear temperature dependence: $S_b^2(T)\propto\tau$. Therefore, the value $S_b^2(T)\tau^{-1}$ is of the order $O(1)$ and in the limit $T\to T_{\mathrm{SDW}}$ the function $\Delta c_{ii}^{(1)}(T)$ is also finite. The transition from $\Delta c_{ii}^{(1)}=0$ to the value $\Delta c_{ii}^{(1)}(T\to T_{\mathrm{SDW}})\neq 0$ takes place in a very narrow temperature interval below T_{SDW} and appears as a jump. Because a change in the sound velocity Δv_l is proportional to $\Delta c_{ii}^{(1)}$, the velocity of the longitudinal acoustic waves also undergoes a jump at T_{SDW}. The jump may be different for longitudinal waves moving along different axes, since the coupling constants G_b^a, G_b^b and G_b^c can be different.

It is interesting to note that the temperature behavior of the susceptibility $[\chi_{bb}(\mathbf{Q},0)\propto|T_{\mathrm{SDW}}-T|^{-1}]$ and the order parameter $[S_b^2(T)\propto(T_{\mathrm{SDW}}-T)]$ corresponds to the conventional mean-field behavior for a second order phase transition. The reason for this fact has been discussed for the itinerant quasi-one-dimensional conductor $(\mathrm{TMTSF})_2\mathrm{PF}_6$.[38]

Now we study the sound attenuation $\alpha_{ii}^{(1)}$. Substituting Eq. (12) into Eq. (10) gives

$$\alpha_{ii}^{(1)}=\left(\frac{4(G_b^i)^2S_b^2(T)A}{Mv_l^3\tau}\right)\frac{\omega_q^2t}{1+\omega_q^2t^2}. \tag{15}$$

Since the value in the brackets is a smooth function of T, the temperature dependence of $\alpha_{ii}^{(1)}$ near T_{SDW} is determined by the characteristic time $t=t_0\tau^{-1}$. It is easy to see that Eq. (15) looks like the standard Debye relaxation results that describe the anomalous sound attenuation due to slow critical fluctuations near the critical temperature of a second order phase transition.[42] According to Eq. (10) one can expect a sharp peak in the attenuation at the temperature determined by the equation $t\omega_q=1$, which is slightly below T_{SDW}. It is interesting to note, that according to Eqs. (14a) and (14b), the elastic constant $\Delta c_{ii}^{(1)}$ reaches the midpoint of the jump at this temperature. By expanding the temperature scale of Fig. 3 (not shown), we verified that this is indeed the case in our experiment.

Now we study the temperature behavior of the fluctuation contributions $\Delta c_{ii}^{(2)}$ and $\alpha_{ii}^{(2)}$ at $T\geqslant T_{\mathrm{SDW}}$. For this purpose it is necessary to calculate the real and imaginary parts of the function $Y_{ij}(q,\omega_q)$ given by Eq. (9). There are two contributions to $Y_{ij}(q,\omega_q)$ which differ in their temperature behavior. The integration in Eq. (9) over the regions far from the points $\mathbf{k}=\pm\mathbf{Q}$ and $\omega=0$ gives a regular function of T denoted as $Y_{ij,r}(q,\omega_q)$, whereas at T close to T_{SDW} the integration in the neighborhood of the points $\mathbf{k}=\pm\mathbf{Q}$ and $\omega=0$ can give a singular function of T which we denote as $Y_{ij,s}(q,\omega_q)$. It is very difficult to calculate the $Y_{ij,r}(q,\omega_q)$, but the singular function $Y_{ij,s}(q,\omega_q)$ may be easily found. For simplicity we neglect the magnetic anisotropy and suppose that $\chi_{ii}(\mathbf{k},\omega)$ for all i is given by Eqs. (12) and (13), then one obtains

$$Y''_{ii,s}(q,\omega_q)=\frac{T\omega_qA^2}{2\pi^3t_0\tau^{3/2}}\left(\frac{d_ad_bd_c}{\xi_{0,a}\xi_{0,b}\xi_{0,c}}\right)\int_{-\infty}^{\infty}\frac{k^2dkd\varepsilon}{[(1+k^2)^2+\varepsilon^2]^2}, \tag{16}$$

$$Y'_{ii,s}(q,\omega_q)=\frac{2TAB}{\pi^3 t_0\tau^{1/2}}\left(\frac{d_a d_b d_c}{\xi_{0,a}\xi_{0,b}\xi_{0,c}}\right)\int_{-\infty}^{\infty}\frac{(1+k^2)k^2 dk d\varepsilon}{[(1+k^2)^2+\varepsilon^2]^2}, \tag{17}$$

i.e., at $T\to T_{\mathrm{SDW}}$ these functions diverge: $Y''_{ii,s}(q,\omega_q)\propto\tau^{-3/2}$ and $Y'_{ii,s}(q,\omega_q)\propto\tau^{-1/2}$. Now from Eqs. (8) and (11) one can find $\Delta c^{(2)}_{ii,s}$ and $\alpha^{(2)}_{ii,s}$. The power law behavior $\alpha^{(2)}_{ii,s}\propto\tau^{-\rho}$ with $\rho=3/2$ is in agreement with Schwabl's result[43] for magnets $\rho=2-v(d-z)$ if we take the mean field values $v=1/2$ and $z=2$ at $d=3$ (the critical exponents are taken from the analysis of NMR data[38]). The comparison of the quantities with the jump $\Delta c^{(1)}_{ii}(T)$ given by Eq. (14a) and $\max\alpha^{(1)}_{ii}$ yields

$$\frac{\Delta c^{(2)}_{ii,s}}{\Delta c^{(1)}_{ii}(T)}\propto\frac{T_c\tau^{-1/2}}{g_2}\left(\frac{d_a d_b d_c}{\xi_{0,a}\xi_{0,b}\xi_{0,c}}\right)<\tau^{-1/2}10^{-4}, \tag{18}$$

$$\frac{\alpha^{(2)}_{ii,s}}{\max\alpha^{(1)}_{ii}}\propto\frac{T_c\tau^{-3/2}t_0\omega_q}{g_2}\left(\frac{d_a d_b d_c}{\xi_{0,a}\xi_{0,b}\xi_{0,c}}\right)<\tau^{-3/2}10^{-6}, \tag{19}$$

where g_2 is the conventional exchange constant (see, for example, Ref. 1) and d_a, d_b, and d_c are the lattice constants. For the estimate we used $\xi_{0,i}\approx 0.46 t_i d_i/T$, and $t_a\approx 3000\,\mathrm{K}\approx 15 t_b\approx 450 t_c$.[3,38] The value $t_0\omega_q\approx 10^{-2}$ we found from the analysis of our data (see the next section). These estimates show that the singular contributions $\Delta c^{(2)}_{ii,s}$ and $\alpha^{(2)}_{ii,s}$ are very small even close to T_{SDW}. Our experimental data for mode II in Fig. 3 is in agreement with the theoretical estimate. A smoothing of the temperature behavior of the sound velocity and attenuation near T_{SDW} that is a fingerprint of fluctuations is not noticeable in Fig. 3.

Summing up, we conclude that the longitudinal modes propagating along the *a*, *b*, and *c* axes exhibit a jump of the velocity at T_{SDW} and a Landau-Khalatnikov peak in the attenuation slightly below T_{SDW}. These longitudinal sound modes we call ''mode II.''

Now we study a transverse acoustic mode which is polarized along the *a* axis and propagating along the *b* axis. It is interesting to note that according to Virosztek and Maki[14] this sound wave couples to the phason of the SDW, and for which one should expect a significant electromechanical effect. Within our model the transverse wave couples to the SDW in the following way:

$$E_t(\varepsilon_{ba})=\sum_{\mathbf{k},\mathbf{q}} G_{ba}\varepsilon_{ba}(\mathbf{q})S_b(\mathbf{k}-\mathbf{q})S_a(-\mathbf{k}). \tag{20}$$

At $T<T_{\mathrm{SDW}}$ we have two contributions into the corresponding elastic constant and the attenuation:

$$\Delta c^{(1)}_{ab}=-(G_{ba})^2 S_b^2(T)\chi'_{aa}(\mathbf{Q}+\mathbf{q},\omega_q), \tag{21}$$

$$\alpha^{(1)}_{ab}=\frac{\omega_q}{M v_t^3}(G_{ba})^2 S_b^2(T)\chi''_{aa}(\mathbf{Q}+\mathbf{q},\omega_q), \tag{22}$$

$$\Delta c^{(2)}_{ab}=-2(G_{ab})^2 Y'_{ab}(q,\omega_q), \tag{23}$$

$$\alpha^{(2)}_{ab}=\frac{2\omega_q}{M v_t^3}(G_{ab})^2 Y''_{ab}(q,\omega_q), \tag{24}$$

where v_t is the velocity of the transverse acoustic wave. Below T_{SDW} the transverse susceptibility $\chi_{aa}(\mathbf{Q}+\mathbf{q},\omega)$ entering into these equations, is not equal to the longitudinal susceptibility $\chi_{bb}(\mathbf{Q}+\mathbf{q},\omega)$ determined by Eqs. (12) and (13). In the collisionless limit, the poles of the $\chi_{aa}(\mathbf{Q}+\mathbf{q},\omega)$ determine the spectrum of magnon excitations (for an itinerant antiferromagnet, see, for example, Ref. 39). Unfortunately $\chi_{aa}(\mathbf{Q}+\mathbf{q},\omega)$ is unknown, but assuming that it is not too singular, the temperature dependence of the elastic constant change is determined by the factor S_b^2, i.e., the square of the order parameter. Maki and Virosztek[13,14] predict a similar temperature dependence near T_{SDW}, making it difficult for this mode to distinguish between the two contributions.

The transverse acoustic mode polarized along *b* axis and propagating along *c* axis displays another type of temperature behavior. For this mode Virosztek and Maki predicts no collective contribution, because it does not couple to the phason.[14] Within our model the mode couples to electrons in the following way:

$$E_t(\varepsilon_{bc})=\sum_{\mathbf{k},\mathbf{q}} G_{bc}\varepsilon_{bc}(\mathbf{q})S_b(\mathbf{k}-\mathbf{q})S_c(-\mathbf{k}). \tag{25}$$

At $T<T_{\mathrm{SDW}}$ we find

$$\Delta c^{(1)}_{bc}=-(G_{bc})^2 S_b^2(T)\chi'_{cc}(\mathbf{Q}+\mathbf{q},\omega_q), \tag{26}$$

$$\alpha^{(1)}_{bc}=\frac{\omega_q}{2M v_{ls}^3}(G_{bc})^2 S_b^2(T)\chi''_{cc}(\mathbf{Q}+\mathbf{q},\omega_q). \tag{27}$$

The fluctuations also produce additional contributions $\Delta c^{(2)}_{bc}$ and $\alpha^{(2)}_{bc}$ determined by Eqs. (23) and (24) after the replacement of the index *a* by *c*. These contributions are also small enough as well as in the case of the mode II. The *c* axis is the hard magnetic axis. Such a magnetic anisotropy must strongly influence the transverse susceptibility $\chi_{cc}(\mathbf{Q},\omega_q)$. The fact can probably be explained by the magnetic anisotropy in g_2. Based on NMR studies,[38] one can suggest that the susceptibility $\chi_{cc}(\mathbf{Q},0)$ has only a cusp at T_{SDW} but not a divergence. Thus, at $T=T_{\mathrm{SDW}}$ the temperature dependence of the elastic constant (26) should also have a kink in the temperature dependence unlike the modes II which have a jump. Below T_{SDW} Eq. (26) predicts the change of the sound velocity to be proportional to the square of the order parameter. One can say less about the attenuation (27) because the temperature behavior of $\chi''_{cc}(\mathbf{Q},\omega_q)$ is unknown. We shall call this transverse mode ''mode I.''

From the phenomenological point of view[18] a qualitative difference in results for modes I and II is related to a difference in kind of coupling. Formally, in accordance to Eq. (20) there is a linear coupling of the strain ε_{ba} to the order parameter S_b multiplied by the fluctuating spin component S_a. After the integration over fluctuations of S_a one obtains that the free energy contains the following coupling term: $F_{\mathrm{I}}\propto S_b^2\varepsilon_{ba}^2$ while, as we have discussed above, for mode II there is a linear coupling $F_{\mathrm{II}}\propto S_b^2\varepsilon_{bb}$. The factor that is proportional to S_b^2 adds to the effective elastic constant of mode I, and we get Eq. (21).

Finally, we consider a transverse mode propagating along the *c* axis and polarized along the *a* axis. For this mode Maki

and Virosztek[14] predict no contribution from coupling to the phason. Within our model the coupling of the mode to electrons is given by

$$E_t(\varepsilon_{ac})=\sum_{\mathbf{k}} G_{ac}\varepsilon_{ac}(\mathbf{q})S_a(\mathbf{k}-\mathbf{q})S_c(-\mathbf{k}). \tag{28}$$

In this case the terms $\Delta c_{ii}^{(1)}$ and $\alpha_{ii}^{(1)}$ equal zero, because $\langle S_a(\mathbf{r})\rangle=\langle S_c(\mathbf{r})\rangle=0$. Therefore, the corrections to the elastic constant and the attenuation of the transverse mode equal $\Delta c_{ii}^{(2)}$ and $\alpha_{ii}^{(2)}$:

$$\Delta c_{ac}^{(2)}=-2(G_{ac})^2Y'_{ac}(q,\omega_q), \tag{29}$$

$$\alpha_{ii}^{(2)}=\frac{2\omega_q}{Mv_t^3}(G_{ac})^2Y''_{ac}(q,\omega_q). \tag{30}$$

As we have discussed above, due to the magnetic anisotropy, the susceptibility $\chi_{cc}(\mathbf{Q},\omega_q)$ has a cusp at T_{SDW}, but does not diverge. This peculiarity of $\chi_{cc}(\mathbf{Q},\omega_q)$ removes singularities in $Y'_{ac}(q,\omega_q)$ and $Y''_{ac}(q,\omega_q)$. Therefore, $\Delta c_{ii}^{(2)}$ and $\alpha_{ii}^{(2)}$ also are expected to have a break in the temperature dependencies at T_{SDW}. This mode we shall call ''mode III.''

From the phenomenological point of view the result $\Delta c_{ii}^{(1)}=\alpha_{ii}^{(1)}=0$ means that mode III is decoupled from the order parameter. Indeed, using the interaction (28) after integration over fluctuating spin components S_a and S_c we obtain the following contribution into the free energy: $F_{\mathrm{III}} \propto -Y'_{ac}\varepsilon_{ba}^2$ with nonsingular Y'_{ac}. The factor that is proportional to Y'_{ac} adds to the effective elastic constant and we get Eq. (29). Therefore we can conclude that a qualitative difference in results for models I, II, and III is related to a difference in kind of coupling of the strain produced by the acoustic modes to the order parameter.

As pointed out before, our consideration was based on the orthorhombic symmetry. For the triclinic symmetry the modes I, II, and III are not pure modes. One should expect that acoustic modes in $(TMTSF)_2PF_6$ have a mixed character of behavior.

IV. ANALYSIS OF THE EXPERIMENTAL DATA

A. Sound velocity

First we shall analyze the temperature behavior of different modes when the sound wave is excited along the c^* axis using longitudinal transducers (see Figs. 2 to 4). As we have discussed in Sec. II, due to the low triclinic symmetry, one can expect the presence of one quasilongitudinal and two quasitransverse modes. Let us identify the observed modes, basing on the theoretical results obtained in Sec. III.

The sound velocity of the mode represented in Fig. 2 shows the behavior expected for the mode I, i.e., the transverse mode propagating along the c axis and polarized along the b axis. In this case according to Eq. (26) the change of the sound velocity should be proportional to the square of the order parameter $S_b^2(T)$. From the data in Fig. 2 we extract the background contribution in the sound velocity below T_{SDW} which was found as a low temperature extrapolation of the polynomial fit of the high temperature part of the curve between 12 K and 40 K. From Refs. 9 and 40 we took NMR data representing the static internal field H_{int} associated with the SDW formation. In Fig. 8 we plot the square of the internal field, H_{int}^2, together with the change of ultrasound velocity. In this case there is a good agreement between our data and the NMR results. This correlation between the order parameter and the velocity of the bending mode in the vibrating-reed experiments was found before by Brown *et al.*[9] For comparison, we added the BCS temperature dependence of the order parameter squared.[44] Maki and Virosztek also predict a change of velocity which near T_{SDW} is proportional to the square of the order parameter, in their case originating from a coupling of this sound mode to the phason of the density wave.[13,14] Lacking knowledge of the respective coefficients, at this stage we are unable to separate the various contributions.

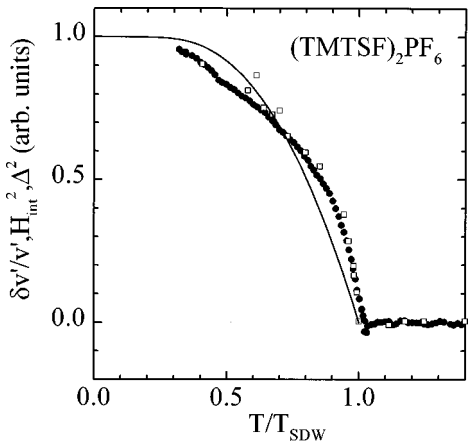

FIG. 8. Comparison of the sound velocity of the mode I (see Fig. 2) behavior below the SDW phase transition with the square of the internal field H_{int}^2 (open squares) at the proton sites that is related to the order parameter squared and the square of the BCS Δ function (solid line). H_{int} is taken from Ref. 40. The temperature background in the sound velocity was subtracted from the data.

Near T_{SDW} the velocity of the mode represented in Fig. 3 has a jump-like behavior which is similar to the predicted behavior for the longitudinal mode II propagating along the c axis [see Eqs. (14a) and (14b)]. Additional evidence for this interpretation comes from the fact that the attenuation has a sharp peak as expected for the longitudinal mode II [see Eq. (15)]. One can see in Fig. 3 that the maximum in the attenuation occurs at the temperature of the midpoint in the sound velocity jump in a complete agreement with our theoretical study of the mode-II behavior. A detailed analysis of the attenuation peak in terms of Eq. (15) will be given below. On decreasing the temperature further, the velocity of this mode behaves similar to the mode I (see Fig. 2). Therefore, the mode in Fig. 3 demonstrates a mixed mode-I–mode-II behavior. Moreover, the main contribution comes from the longitudinal mode II, and a relatively small contribution comes from the transverse modes I. Therefore, the mode in Fig. 3 is a quasilongitudinal sound wave propagating along the c^* axis.

The velocity and the attenuation of the acoustic mode represented in Fig. 4 show only a break in the temperature dependence at the SDW transition. According to our theoretical considerations such a behavior is expected for the sound mode III, i.e., the transverse acoustic wave propagating along the c axis and polarized along the a axis [see Eqs. (29) and (30)].

In the case shown in Fig. 5 the sound wave was excited using transverse transducers with the polarization vector along the *a* axis. Writing the total change of elastic constant as $\Delta c = a_1 \Delta c_1 + a_2 \Delta c_{II} + a_3 \Delta c_{III} + \cdots$, the temperature dependence of the sound velocity displays a mixture of mode I, mode II, and mode III behavior, with a sign reversal for the coefficients of mode I and III.

B. Attenuation of sound

As seen from Figs. 2 to 5, the observed acoustical modes differ in the temperature dependence of the attenuation. Some of them have a peak at temperatures slightly below T_{SDW}. The others have a smooth behavior near the phase transition. There are also significant differences in the low temperature behavior. For these reasons we believe that this is a manifestation of different mechanisms of the sound attenuation.

At first, we study the peak in the attenuation of the sound mode shown in Fig. 3 within our theory. In Sec. IV A, analyzing the sound velocity behavior, we have identified this mode as the quasilongitudinal mode II. In order to check this conclusion let us analyze the form of the peak and its position and compare this with Eq. (15). As it was discussed in Sec. III, the temperature of the maximum is determined by the condition $t\omega_q = 1$. For the used frequency $f = 200\,\mathrm{MHz}$ the condition gives the characteristic time $t = t_0 \tau^{-1} = 8 \times 10^{-10}\,\mathrm{s}$. The maximum is observed about 0.3 K below T_{SDW}. From this we conclude that in $(TMTSF)_2PF_6$ the bare characteristic relaxation time of spin fluctuations along the *b* axis is equal to $t_0 = 2 \times 10^{-11}\,\mathrm{s}$. This value has the same order of magnitude as it was found for other antiferromagnetic systems.[45,46] There should be no fundamental difference between the coupling of local antiferromagnets to the sound waves and an itinerant SDW state. At temperatures above the peak ($t\omega_q \gg 1$) but below T_{SDW}, Eq. (15) can be written in an approximate form:

$$\alpha^{(1)} \approx \alpha_0 / t = \alpha_0 t_0^{-1} (1 - T/T_{SDW}) \equiv \alpha_1 (1 - T/T_{SDW}). \tag{31}$$

On the other hand, at T below the peak when $t\omega_q \ll 1$ we have

$$1/\alpha^{(1)} \approx 1/(\omega^2 t \alpha_0) = (\omega^2 t_0 \alpha_0)^{-1} (1 - T/T_{SDW}) \equiv \alpha_2^{-1} (1 - T/T_{SDW}). \tag{32}$$

Hence, we obtain the following useful relation: $\alpha_2/\alpha_1 = \omega_q^2 t_0^2$ which enables us in another way to find t_0, calculating the slopes of the functions $\alpha^{(1)}$ and $1/\alpha^{(1)}$ in regions of the linear temperature dependence. The existence of a temperature region where $1/\alpha^{(1)}$ has a linear dependence can be seen in Fig. 9 (the data represented by filled squares). Applying this analysis to the attenuation peak displayed in Fig. 3, we obtain $t_0 = 5 \times 10^{-11}\,\mathrm{s}$ in satisfactory agreement with the first estimate. The difference between the two estimates can be related to the fact that apart from the Landau-Khalatnikov mechanism of the sound attenuation there are additional mechanisms that also give temperature dependent contributions. Some of them will be discussed below.

It was shown[47] that the ultrasonic attenuation of the longitudinal waves at an incommensurate phase transition has a peak due to the coupling of the acoustic waves to the phason mode. However, in $(TMTSF)_2PF_6$ the spin-density wave is pinned (see, for example the review[4]) moving the phason mode into the GHz range[6] and we think that the phason mechanism can be excluded.

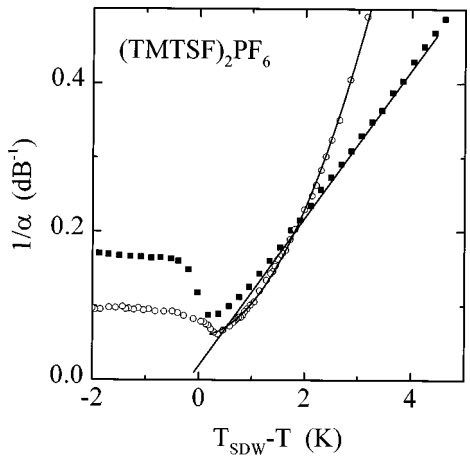

FIG. 9. Inverse attenuation $1/\alpha$ versus T_{SDW}-T: the filled squares correspond to mode II from Fig. 3; the open circles correspond to mode I from Fig. 2. The lines indicate the linear and parabolic behavior, respectively.

The attenuation of the acoustic mode represented in Fig. 2 also has a peak at a temperature slightly below T_{SDW}. However, the peak is more symmetric than the nonsymmetric Landau-Khalatnikov peak in Fig. 3. Moreover, there is no region with linear temperature dependency as discussed above. This can be clearly seen from Fig. 9 where we plot $1/\alpha(\omega)$ versus $T_{SDW} - T$. Above we have classified this acoustic mode as the quasitransverse mode I. To make a detailed analysis of the attenuation peak, it would be necessary to know the staggered susceptibility along the *c* axis.

However, since it is clear that below T_{SDW} we have a strong decrease of the electronic attenuation, we can analyze the behavior of the sound attenuation in Fig. 2 by using a BCS expression with a type II coherence factor appropriate for an SDW[32,48]

$$\frac{\alpha_s}{\alpha_N} = \frac{1}{\hbar\omega} \int_{-\infty}^{\infty} \frac{[E(E+\hbar\omega)+\Delta^2][f(E)-f(E+\hbar\omega)]}{(E^2-\Delta^2)^{1/2}[(E+\hbar\omega)^2-\Delta^2]^{1/2}} dE. \tag{33}$$

Our best fit yields a single particle gap $2\Delta(0) \approx 96\,\mathrm{K}$ (see Fig. 2). In this calculation we used the temperature dependence of the gap extracted from our ultrasonic data (see Sec. IV A and Fig. 8). The obtained value of the energy gap is significantly larger than the prediction of the mean field theory $2\Delta(0) = 3.52 k_B T_{SDW}$ and the result $2\Delta(0) \approx 46\,\mathrm{K}$ determined from transport measurements.[49] Recent optical experiments[50] show a single particle gap $2\Delta(0) \cong 100\,\mathrm{K}$. The discrepancies may be attributed to the dispersion of the energy bands in quasi-one-dimensional compounds with deviations from perfect nesting.[51]

The low temperature behavior of the sound attenuation of the acoustic modes represented in Figs. 3–5 has a power law character unlike the exponential behavior found in Fig. 2. Recently, based on an NMR study on $(TMTSF)_2PF_6$, Valfells *et al.*[20] suggested that the SDW phase transition at

$T_{SDW} \sim 12$ K causes an incomplete opening of the SDW gap and leaves residual carriers at the Fermi surface. These residual carriers can possibly produce the observed power-law temperature behavior of the sound attenuation at $T < T_{SDW}$.[52] However, these assumptions give only a qualitative explanation. A detailed quantitative analysis demands a model of an incomplete SDW transition.

V. DISCUSSION AND CONCLUSION

From our experiments we can conclude that the coupling of the SDW to the lattice is important for both longitudinal and transverse acoustical modes. These findings may explain the problem related to the missing spectral weight of the collective phason excitation observed in the SDW state by optical and dielectric measurements.[6,53] At first glance there should not be any coupling to the lattice and the effective mass of the phason should be unity. The electron-phonon coupling may lead to an enhancement of the effective mass of the SDW condensate. Recently, x-ray diffuse scattering experiments[54] gave indications of a mixed charge-spin character of the modulation in $(TMTSF)_2PF_6$, implying a coupling of the electronic degrees of freedom and the lattice. In further experiments we want to investigate the pinning of the SDW to the lattice by studying the acoustic properties while applying an electric field stronger than the threshold sliding field.

We report high frequency ultrasonic studies of the quasi-one-dimensional organic conductor $(TMTSF)_2PF_6$ below 40 K. We have shown that the sound velocity and the attenuation of sound have a more complicated behavior at the SDW phase transition and in the SDW state, than it was supposed before. For some modes, the sound velocity in the SDW phase changes with temperature as the square of the order parameter. For others, there is a jump in the sound velocity at the critical temperature T_{SDW}. Still another mode shows a kink at T_{SDW} and a slow decrease of the velocity below this temperature. The behavior of the attenuation is also different for different modes. One of them exhibits a Landau-Khalatnikov-like peak with a characteristic relaxation time $t_0 = 2 \times 10^{-11}$ s. Another one shows a BCS-like behavior in the SDW state with an energy gap value equal to $2\Delta(0) \approx 96$ K. A phase transition between different SDW states at 3.5 K manifests itself as a kink in the temperature dependence of the sound velocity. Moreover, an additional term which appears in the sound velocity below 3.5 K shows a linear temperature dependence in the low temperature phase. Our results for the influence of an applied magnetic field along the c^* axis on the SDW phase transition are consistent with earlier works.

Our theoretical consideration of the experimental results was based on the assumption that phonons influence the exchange interactions between spins of conduction electrons and couple to the spin-density wave in accordance to Eq. (3). Within the proposed model we have found that the temperature behavior of the sound velocity and the attenuation of sound is related to the real and imaginary parts of the dynamical spin susceptibility. In this way different types of temperature dependencies may be explained when taking into account the magnetic anisotropy. For example, the attenuation of the longitudinal mode propagating along the c axis is related to the imaginary part of the longitudinal susceptibility along the easy axis, whereas the jump in the velocity is related to the real part of the susceptibility. The temperature behavior of a transverse sound wave propagating along the c axis with polarization along the a or b axes is determined by the transverse susceptibility. Therefore, we find acoustic measurements to be a powerful instrument for investigating $(TMTSF)_2PF_6$, and, in addition to NMR measurements which give information about the imaginary part of the dynamical susceptibility, the acoustic measurements enable us to investigate both real and imaginary parts of the dynamical susceptibility.

ACKNOWLEDGMENTS

This work was supported by SFB 252. The work at UCLA was supported by NSF Grant No. 9503009. S.Z. would like to thank the Alexander von Humboldt Foundation for financial support. One of the authors (A.G.) gratefully acknowledges the Physics Institute of the Frankfurt University for hospitality as well as the Russian Fund of Fundamental Investigations for the financial support in part under Grant No. 98-02-18299. We thank Professor B. Lüthi for some fruitful discussions and criticisms.

[1] J. Solyom, Adv. Phys. **28**, 201 (1979).
[2] V. J. Emery, in *Highly Conducting One-Dimensional Solids*, edited by J. T. Devreese, R. P. Evrard, and V. E. van Doren (Plenum, New York, 1979).
[3] D. Jérome and H. J. Schulz, Adv. Phys. **31**, 299 (1982).
[4] D. Jérome, in *Organic Conductors*, edited by J.-P. Farges (Dekker, New York, 1994).
[5] G. Creuzet, C. Gaonach, and B. Hamzic, Synth. Met. **19**, 245 (1987).
[6] S. Donovan, Y. Kim, L. Degiorgi, M. Dressel, G. Grüner, and W. Wonneberger, Phys. Rev. B **49**, 3363 (1994).
[7] P. M. Chaikin, T. Tiedje, and A. N. Bloch, Solid State Commun. **10**, 739 (1982).
[8] S. E. Brown, B. Alavi, G. Grüner, and K. Bartholomew, Phys. Rev. B **46**, 10 483 (1992).
[9] S. E. Brown, B. Alavi, W. G. Clark, M. E. Hanson, and B. Klemme, J. Phys. IV **3**, C2-225 (1993).
[10] X. D. Shi, L. Chiang, and P. Chaikin, in *Advanced Organic Solid State Materials*, edited by L. Y. Chiang, P. Chaikin, and D. O. Cowan, MRS Symposia Proceedings No. 173 (Materials Research Society, Pittsburgh, 1990), p. 239.
[11] Z. G. Xu, G. Minton, J. W. Brill, T. Burgin, and L. K. Montgomery, Synth. Met. **56**, 2797 (1993).
[12] K. Maki and A. Virosztek, Phys. Rev. B **36**, 2910 (1987).
[13] K. Maki and A. Virosztek, Synth. Met. **29**, F371 (1989).
[14] A. Virosztek and K. Maki, Phys. Rev. B **53**, 3741 (1996).
[15] B. Lüthi, G. Bruls, P. Thalmeier, B. Wolf, D. Finsterbusch, and I. Kouroudis, J. Low Temp. Phys. **95**, 257 (1994).
[16] R. Truell, C. Elbaum, and B. Chick, *Ultrasonic Methods in Solid State Physics* (Academic, New York and London, 1969).

[17] F. E. Borgnis, Phys. Rev. **98**, 1000 (1955).
[18] W. Rehwald, Adv. Phys. **22**, 721 (1973).
[19] J. W. Brill, M. Chung, Y.-K. Kuo, X. Zhang, and E. Figueroa, Phys. Rev. Lett. **74**, 1182 (1995).
[20] S. Valfells, P. Kuhns, A. Kleinhammes, J. S. Brooks, W. Moulton, S. Takasaki, J. Yamada, and H. Anzai, Phys. Rev. B **56**, 2585 (1997).
[21] S. Uji, J. S. Brooks, M. Chaparala, S. Takasaki, J. Yamada, and H. Anzai, Phys. Rev. B **55**, 12 446 (1997).
[22] H. J. Pederson, J. C. Scott, and K. Bechgaard, Solid State Commun. **35**, 207 (1980).
[23] M. Dumm, M. Dressel, and A. Loidl (unpublished).
[24] G. Kriza, G. Quirion, O. Traetteberg, and D. Jérome, Europhys. Lett. **16**, 585 (1991).
[25] G. Kriza and O. Traetteberg, J. Phys. IV **3**, C2-15 (1993).
[26] L. C. Lasjaunias, K. Biljakovic, and P. Monceau, Phys. Rev. B **53**, 7699 (1996).
[27] F. Nad, P. Monceau, and K. Bechgaard, Solid State Commun. **95**, 655 (1995).
[28] L. C. Lasjaunias, K. Biljakovic, F. Nad, P. Monceau, and K. Bechgaard, Phys. Rev. Lett. **72**, 1283 (1994).
[29] G. M. Danner, P. M. Chaikin, and S. T. Hannahs, Phys. Rev. B **53**, 2727 (1996).
[30] N. Biskup, S. Tomic, and D. Jérome, Phys. Rev. B **51**, 17 972 (1995).
[31] A. Bjelis and K. Maki, Phys. Rev. B **45**, 12 887 (1992).
[32] G. Grüner, *Density Wave in Solids* (Addison-Wesley, Reading, MA, 1994).
[33] K. Mortensen, Y. Tomkiewicz, and K. Bechgaard, Phys. Rev. B **25**, 3319 (1982).
[34] C. Herring, in *Magnetism*, edited by G. T. Rado and H. Suhl (Academic, New York, 1966), Vol. IV.
[35] P. Thalmeier and B. Lüthi, in *Handbook on the Physics and Chemistry of Rare Earths*, edited by K. A. Gschneidner, Jr. and LeRoy Eyring (North-Holland, Amsterdam, 1991), Vol. 14.
[36] E. R. Callen and H. B. Callen, Phys. Rev. **129**, 578 (1963).
[37] G. Grüner, Rev. Mod. Phys. **66**, 1 (1994).
[38] C. Bourbonnais, P. Stein, D. Jérome, and Moradpour, Phys. Rev. B **33**, 7608 (1986).
[39] S. H. Liu, Phys. Rev. B **2**, 2664 (1970).
[40] W. G. Clark, M. E. Hanson, W. H. Wong, and B. Alavi, Physica B **194-196**, 285 (1994).
[41] T. Takahashi, Y. Maniwa, H. Kawamura, and G. Saito, J. Phys. Soc. Jpn. **55**, 1364 (1986).
[42] L. D. Landau and I. Khalatnikov, Dokl. Akad. Nauk SSSR **96**, 469 (1954).
[43] F. Schwabl, Phys. Rev. B **7**, 2038 (1973).
[44] B. Mühlschlegel, Z. Phys. **155**, 313 (1959).
[45] T. J. Moran and B. Lüthi, Phys. Rev. B **4**, 122 (1971).
[46] A. Bachellerie, J. Joffrin, and A. Levelut, Phys. Rev. Lett. **30**, 617 (1973).
[47] A. M. Schorgg and F. Schwabl, Phys. Rev. B **49**, 11 682 (1994).
[48] M. Tinkham, *Introduction to Superconductivity* (McGraw-Hill, New York, 1994).
[49] G. Mihály, Y. Kim, and G. Grüner, Phys. Rev. Lett. **67**, 2713 (1991).
[50] L. Degiorgi, M. Dressel, A. Schwartz, B. Alavi, and G. Grüner, Phys. Rev. Lett. **76**, 3838 (1996).
[51] G. Mihály, A. Virosztek, and G. Grüner, Phys. Rev. B **55**, 13 456 (1997).
[52] J. Moreno and P. Coleman, Phys. Rev. B **53**, R2995 (1996).
[53] G. Mihály, Y. Kim, and G. Grüner, Phys. Rev. Lett. **66**, 2806 (1991).
[54] J. P. Pouget and S. Ravy, J. Phys. I **6**, 1501 (1996).